Journal of Marine Research, 67, 701–729, 2009

Journal of
MARINE RESEARCH

Volume 67, Number 6

Effects of surface forcing on the seasonal cycle of the eastern equatorial Pacific

by D. E. Harrison,[1] A. M. Chiodi[1,2] and G. A. Vecchi[1,3]

ABSTRACT

The roles of zonal and meridional wind stress and of surface heat flux in the seasonal cycle of sea surface temperature (SST) are examined with a primitive equation (PE) model of the tropical Pacific Ocean. While a variety of previous numerical and observational studies have examined the seasonal cycle of SST in the eastern tropical Pacific, it is noteworthy that different mechanisms have been invoked as primary in each case and different conclusions have been reached regarding the relative importance of the various components of surface forcing. Here, we perform a series of numerical experiments in which different components of the surface forcing are eliminated and the resulting upper ocean variability is compared with that of the climatological experiment. The model used for these experiments reproduces a realistic climatological seasonal cycle, in which SST emerges as an independent quantity. We find that the different cases all produce qualitatively reasonable seasonal cycles of SST, though only the most complete model is also able to reproduce the seasonal cycle of near surface currents, tropical instability waves (TIWs), and net surface heat fluxes consistent with historical observations. These results indicate that simply reproducing a qualitatively accurate seasonal cycle of SST does not necessarily allow meaningful conclusions to be made about the relative importance of the different components of surface forcing. The results described here also suggest that a model simulation must at least reproduce all the documented near surface kinematic features of the equatorial Pacific cold tongue region reasonably well, before accurate inferences can be made from model experiments. This provides useful guidelines to current efforts to develop and evaluate more complex fully coupled air-sea models and shows that results for simple or intermediate ocean models that do not have this level of fidelity to the observations will be difficult to interpret.

1. NOAA/PMEL, 7600 Sand Point Way, Seattle, Washington, 98115, U.S.A.
2. Corresponding author. ***email: andy.chiodi@noaa.gov***
3. Present address: Geophysical Fluid Dynamics Laboratory, NOAA, Princeton, New Jersey, 08542, U.S.A.

1. Introduction

The seasonal cycle and interannual variation of tropical Pacific SST has been the focus of considerable research, as work continues to try to understand and to predict the El Niño-Southern Oscillation (ENSO) phenomenon. The known influence of ENSO on global seasonal climate anomalies makes it, and by association, the seasonal cycle of SST, much scrutinized features of global coupled models that are currently under development and evaluation (e.g., de Szoeke and Xie, 2008).

It has long been known that the eastern equatorial Pacific exhibits a strong annual cycle in SST (range of about 5°C; peak in March) and a much weaker semi-annual cycle (range of about 0.5°C; see Levitus, 1987). Unlike most ocean regions, however, the relative strengths of these cycles in the equatorial Pacific cannot be explained by local top-of-the-atmosphere solar radiation variability which is dominated by the semi-annual cycle at the equator (downward peaks at the March and September equinoxes). Thus, the relatively strong annual cycle of SST in the eastern equatorial Pacific must predominantly arise from something other than the local effects of seasonal changes in sun-earth orbital geometry.

Since SST is the primary oceanic variable that affects the atmosphere, there has been much interest in trying to understand its variations. Efforts to model seasonal and interannual SST changes have been made with ocean and coupled air-sea models of different levels of complexity (discussed in detail below).

The different models encourage analyses of upper ocean temperature variability to be done in different ways and, where direct comparison of results is possible, this seems to produce different results. In the context of the high resolution PE model, results of heat (or temperature) budget analyses are particularly sensitive to the depth over which averaging is done to define SST (e.g., a choice of 20 m often yields quite different results from one of 50 m) and often have substantially different character depending on geographic location (e.g., Borovikov, 2000). Results also appear to be sensitive to the near surface configuration of the ocean model (e.g., Chen *et al.*, 1994a). Rigorous analyses of the involved ocean processes (e.g., term balances) and model configuration effects are beyond the scope of this work. Instead, an approach is offered to examine the effects of various surface forcing components on the aspects of the upper ocean seasonal cycle that can be confirmed by observations, especially SST.

Surface heat flux depends on the SST as well as atmospheric variables such as wind speed, air temperature and humidity and cloud cover. Fully coupled air-sea models allow for the simultaneous computation of SST and these atmospheric variables. Such coupled models are under development (Wittenberg *et al.*, 2006; Cai, 2002; Schneider, 2002; Perigaud *et al.*, 2000; DeWitt and Schneider, 1999; Delecluse *et al.*, 1998; Robertson *et al.*, 1995), and have achieved some measure of success (de Szoeke and Xie, 2008; Guilyardi, 2006; Davey *et al.*, 2002; Latif *et al.*, 2001; Mechoso *et al.*, 1995), though certain problems, such as finding a physically realistic parameterization of atmospheric convection and cloud cover persist (Arakawa, 2004). Coupled models provide a consistent set of surface fluxes and SST, but the upper ocean variability predicted in such models is often significantly

influenced by wind stress errors produced from the atmospheric model (e.g., de Szoeke and Xie, 2008; DeWitt and Schneider, 1999). Also, the computational costs associated with the fully coupled models often prevent multiple deterministic experiments from being run, as is done here. Thus, this study is complementary to current efforts to improve the simulation of the seasonal cycle of SST and ENSO in fully coupled models, such as those submitted for inclusion in the recent Intergovernmental Panel on Climate Change Fourth Assessment Report (IPCC AR4).

To examine the surface forcing mechanisms for the seasonal cycle of SST in the eastern equatorial Pacific, we use an ocean model forced with observed winds and surface heat fluxes that are specified from the model SST and an imposed climatological atmosphere. Since we wish to determine the effects of ocean currents from our model simulations, and ocean currents are driven by winds, using observed wind stress fields is possibly advantageous in this case. On the other hand, care must be taken that the imposed surface heat flux condition does not introduce inconsistencies between oceanic heat advection and surface heat flux, as described by Seager *et al.* (1995a). To do this, we specify as a "compatibility" condition that any computed parameters that figure into the surface boundary with the atmosphere, that are not imposed directly (e.g., SST, surface heat flux), must be consistent with data.[4] A model that produces realistic currents, a realistic vertical density structure, and atmospheric parameters that are in "the ballpark" or better may be said to be self-consistent. It is sensible and meaningful to use subsurface velocity and temperature fields from such a model to speculate about oceanic balances and processes. So long as the model's temperature gradient fields agree with observations, it is reasonable to diagnose the role of ocean advection in a PE ocean model that integrates observed wind stress. The subsurface conditions are what is obtained from this exercise, and they are, after all, the things that are the most difficult to measure.

However the near-surface temperature budgets are done, no simple story has evolved to explain how the Pacific warms and cools (either seasonally or interannually), except in the early ocean warming stage of ENSO events (when anomalous zonal advection appears to be a primary warming mechanism, driven either by local or remote reductions in the easterlies). In the seasonal cycle, SST variations appear to result from small imbalances among much larger heat equation terms, particularly nonlinear advection, surface heat flux and vertical mixing. But can we say what combination of circumstances (model and boundary conditions) together make analysis of processes affecting SST meaningful? And if we can reach this state, what can we say about where we are right now in our understanding of these processes?

In this study, the roles of zonal and meridional wind stress, as well as surface heat fluxes, in the upper ocean seasonal cycle are explored with a physically realistic PE model of the

4. In the absence of a complete coupled model, imposition of a more complicated surface heat flux boundary condition to an ocean model (e.g., Kessler *et al.*, 1998; Seager *et al.*, 1988) does not change this. Rather it just creates a more subtle compatibility condition.

Table 1. Summary of numerical model studies of the seasonal cycle of the eastern tropical Pacific Ocean. The type of model used, the forcing imposed at the surface, and the conclusion about what primarily drives the seasonal cycles of SST are listed for each study. While the seasonal cycle of SST is reproduced quite credibly in every case, the forcing and the conclusions reached vary widely.

Authors	Date	Model Used	Forcing Used	Conclusions Reached
Philander and Pacanowski	1981	PE(MOM)	idealized meridional wind stress; no zonal wind stress; surface heat flux proportional to difference between SST and reference temperature	meridional stress alone produces SST seasonal cycle, including cold tongue
Takeuchi	1986	Bryan-type 10-level PE model	seasonal wind stress forcing; Haney-type surface heat flux parameterization was employed; heat flux is proportional to the difference between SST and a reference	equatorial upwelling does not contribute to SST seasonal cycle; cold water tongue is supplied by meridional wind stress-forced upwelling and temperature advection along the eastern boundary; westward surface currents carry cold water westward along the equator
Seager *et al.*	1988	linear $1\frac{1}{2}$-layer model for velocity; nonlinear temperature equation in the upper layer	seasonal wind stress forcing; sensible heat flux proportional to the difference between SST and a reference temperature: latent heat flux parameterized with the surface wind and SST; solar heating a function of cloud cover and latitude	cold tongue is primarily due to variations of cloud cover; strong equatorial upwelling yields cooling, zonal and meridional advection have significant effects only when the cold tongue is most developed
Köberle and Philander	1994	PE(MOM)	seasonal wind stress forcing; heat fluxes from bulk formula model SST and observed atmospheric fields	eastern equatorial SST seasonal cycle controlled by local wind-induced upwelling and modulation of upwelling by surface heat fluxes
Chang	1994	$1\frac{1}{2}$-layer reduced gravity model for velocity; two mixed layer configurations	seasonal wind stress forcing; climatological heat flux forcing with surface relaxation to climatological SST	wind-driven ocean dynamics and surface heat flux forcing are important to the eastern equatorial SST seasonal cycle; response to heat flux forcing is larger for variable mixed layer depth case; westward propagations of equatorial seasonal cycle depends on dynamical response to wind; unclear if meridional or zonal component dominates

Chen *et al.*	1994	reduced gravity PE model; variable depth mixed layer with hybrid mixing; 8 lower sigma layers	seasonal wind stress forcing; heat flux as in Seager (1988)	annual cycle of SST in eastern equatorial Pacific controlled largely by annually varying mixed layer depth; mixed layer depth controlled by solar forcing and wind mixing
Li and Philander	1996	Cane-Zebiak type ocean coupled to Lindzen-Nigam atmosphere	specified time average conditions; specified solar forcing; surface solar forcing depends on SST via cloud parameterization; latent heat flux from model SST, winds and empirically determined-near surface humidity	eastern equatorial SST seasonal cycle driven mainly from effects of meridional winds on asymmetric mean state; effects of meridional ocean advection and meridional wind-induced latent heat flux variability mainly drive annual cycle, with some contribution from cloud effects on solar forcing
Chang	1996	Cane-Zebiak type ocean coupled to Lindzen-Nigam atmosphere	specified time average conditions; seasonally varying solar forcing assuming constant cloudiness	eastern equatorial SST seasonal cycle influenced by zonal and meridional coupling; strong annual SST signal in near-coastal region mainly from meridional coupling; westward expansion of signal from zonal interactions
Kessler *et al.*	1998	sigma-layer tropical PE GCM	seasonal wind stress forcing; heat flux computed from only cloud cover and wind speed; solar radiation was modulated by cloud fraction and adjusted empirically	SST seasonal cycle can be described as simply following the variation of net solar radiation at the sea surface
Borovikov *et al.*	2000	reduced gravity quasi-isopycnal model	seasonal wind stress forcing; heat fluxes from Seager (1995b) methods; specified air temperature, humidity, solar forcing and cloud cover	character of surface heat budget highly dependent on longitude; no simple explanation for seasonal cycle; details of heat budgets depend on wind stress used
Fu and Wang	2001	$2\frac{1}{2}$-layer PE atmospheric model, coupled to an ocean with mixed layer, thermocline and motionless deep layer	fully coupled forcing over the tropical Pacific, except cloud amounts are specified for longwave and shortwave radiation	Seasonal cycle of SST in in the eastern equatorial Pacific is primarily due to the effects of meridional wind on entrainment and latent heat flux

Pacific that is among the most complex in use. The climatological seasonal cycle experiment described by Harrison *et al.* (2000) is the starting point for a series of numerical experiments in which different components of the surface forcing are eliminated and the resulting upper ocean variability is compared with that of the climatological experiment. The wind fields used are always based on the climatological wind stress field of the tropical Pacific. We examine the relative importance of the surface heat flux, and zonal and meridional wind stress in driving the near-surface seasonal cycle in the extreme eastern Pacific (east of 95°W), in the western Pacific (west of the dateline) and in the predominant trade wind region (95°W–180°W). Previous numerical and observational work is examined in Section 2, with a summary of the numerical work given in Table 1. Our numerical model is described in Section 3. Because the surface heat flux boundary condition is critical in this context, in Section 3 we discuss the role of our surface heat flux boundary condition in the near-surface heat equation. In Section 4 we compare the results from a series of numerical experiments, and in Section 5 a discussion of the main results is given.

2. Background

a. Numerical model experiments

In an attempt to gain insight into the surface forcing processes that control SST evolution (especially meridional wind stress), Philander and Pacanowski (1981) carried out a numerical study using idealized meridional wind stress patterns, with no zonal wind stress. The numerical model was the same PE model as is used here, but used a rectangular domain with an idealized density field, slightly different parametrization for horizontal diffusion and surface heat flux proportional to the difference between SST and a reference temperature (25°C). They found that a modest equatorial cold tongue could be produced with a constant meridional stress field. Confining wind stress to the eastern part of the basin and adding a periodic component produced some variation in equatorial and near-"coastal" SST while maintaining a cold tongue. They inferred that "SST variations observed in the eastern equatorial Pacific Ocean on seasonal time scales may, to a large extent, be due to the variability of the local meridional winds," i.e., meridional stress alone may be a substantial factor in both seasonal and interannual SST variation in the equatorial eastern Pacific. A similar model was later used by Philander *et al.* (1987) to study upper tropical Pacific circulation. In this case, both components of wind stress were applied to the model.

Takeuchi (1986) studied the seasonal variability of cold surface water in the eastern tropical Pacific ("cold tongue") with a Bryan-type 10-level PE model (Bryan, 1969; see also Gordon and Corry, 1991). Also in this case, a Haney-type surface heat flux parameterization was employed (Haney, 1971), where the heat flux is proportional to the difference between SST and a constant reference temperature. There was no seasonal variation in thermal forcing; the only seasonal forcing was supplied by the wind stress. Based on his model results, Takeuchi concluded that "the main portion of the cold water tongue is supplied by meridional wind stress-forced upwelling along the eastern boundary several hundred

km south of the equator. The upwelled water is advected equatorward along the coast, the cold water then extends westward along the equator carried by strong westward surface currents. It is a rather surprising conclusion that equatorial upwelling does not contribute to the seasonal variation of SST."

Seager *et al.* (1988) studied the tropical Pacific SST climatology with a simplified linear 1 1/2-layer model for velocity (but with a nonlinear temperature equation in the upper layer) which used a surface heat flux parameterization that does not include air temperature and humidity. As with several of the other model studies mentioned here, the sensible heat flux in this case was proportional to the difference between SST and a reference temperature. Latent heat flux was parameterized with the surface wind and SST, and solar heating was specified as a function of cloud cover, latitude and (constant) surface albedo. The major elements of the seasonal development of the SST field were seen in the model results. The authors reported that the cold tongue is primarily due to a maximum of cloud cover which induces a minimum of surface heating, and stated that "during northern hemisphere fall, when the SST is a minimum, there is a strong cooling due to (equatorial) upwelling, which overpowers the surface heating."

Motivated by reports from Seager and Blumenthal (1994) that, in the Cane-type model (Cane, 1979) described by them, "inadequate treatment of mixed layer/entrainment processes in upwelling regions of the eastern tropical Pacific leads to a large and seasonally varying error in the model SST," Chen *et al.* (1994b) used an ocean model configured with a variable depth well-mixed upper layer and several deeper isopycnal layers to study the seasonal cycle of SST in the tropical Pacific. In this case, surface fluxes were specified according to the method of Seager *et al.* (1988). Chen *et al.* (1994b) emphasized the importance of ocean mixing processes, reporting that "It is found that the large SST annual cycle in the eastern equatorial Pacific is, to a large extent, controlled by the annually varying mixed layer depth which, in turn, is mainly determined by the competing effects of solar radiation and wind forcing." The effects of upper ocean model configuration were also discussed by Chang (1994).

Köberle and Philander (1994, KP94 hereafter) studied the processes that control seasonal SST variation in the tropical Pacific (20°S to 20°N) with a PE model similar to the one used here. Seasonally varying wind stress and surface heat flux was applied to the model based on climatological atmospheric conditions and model SST. It was found that this model generally reproduced realistic seasonal SST variations when all surface forcing components were applied. Experiments, similar to some described in the present study, were then performed in which the seasonal variations were alternately removed from surface heat flux and wind stress fields prior to model integration. Effects of these perturbations varied with location, but analysis of the upper ocean (0–50 m depth) heat budget in the eastern equatorial Pacific (defined in this case as 4°S to 4°N and 104°W to 86°S) led authors to conclude that, essentially, "…the seasonal cycle variations in heat flux are balanced by seasonal variations in the upwelling of a steady stratification plus the steady upwelling of a seasonally varying stratification." In this case, the seasonally varying stratification was caused by "heat fluxes

that modulate mixing processes in the ocean," as opposed to thermocline depth variations which were said to play a more important role in causing interannual SST variability. The authors also conclude that elsewhere in the study region, the upper ocean seasonal cycle is essentially caused by net surface heating. Experiments described in the present study revisit the relationship between effects of surface heat and momentum fluxes, but expand upon the study of KP94 by separately considering the effects of zonal and meridional components of wind stress. This was not done in KP94. Also, unlike KP94, the present study focuses only on the near-equatorial region, where oceanic Kelvin waves are prominent features of ocean adjustment to wind stress variations. The conclusions reached in the present study (discussed below) are in many respects different from those reached by KP94.

Li and Philander (1996) report results from a simple, coupled ocean-atmosphere model, consisting of a Lindzen-Nigam type atmosphere (Lindzen and Nigam, 1987) coupled to a Cane-Zebiak type ocean model (Cane, 1979; Zebiak and Cane, 1987; see also Chang (1996) for a study using a similar model). Theirs is an anomaly model forced by incoming solar radiation with cloud fraction specified as a simple function of model SST. Experiments were performed that depended on splitting the solar forcing and time-mean model states in to parts symmetric and asymmetric about the equator. The authors concluded that the asymmetric state is mainly responsible for the strong annual cycle of SST in the equatorial Pacific; because of time-mean meridional contrasts in eastern equatorial Pacific SST, "the northward winds at the equator will be intense toward the end of the northern summer, relaxed toward the end of southern summer." In their model, modulation of evaporation by these meridional winds drives an annual cycle of SST at the equator of modest amplitude, that "can be augmented by next taking into account the dynamical response of the ocean to the winds." It was also found that the seasonal cycle in eastern equatorial SST is augmented by seasonal changes in cloud cover predicted by the model. Interested readers can also consult Giese and Carton (1994) for another coupled-model perspective. In this case, it was concluded that the coupled Pacific system has a "timescale that allows the annual cycle to be amplified preferentially."

Kessler *et al.* (1998; K98 hereafter) report results from an upper ocean general circulation model (GCM) of the tropical Pacific. The model consists of a surface wind-forced sigma-layer tropical PE GCM developed by Gent and Cane (1989), with a surface mixed layer formulation developed by Chen *et al.* (1994a,b) (see also Kraus and Turner (1967) and Price *et al.* (1986)) as its upper layer. Their surface heat flux boundary condition was based on the heat flux formulation of Seager *et al.* (1988), which requires only cloud cover and wind speed as input. Solar radiation intensity was modulated by cloud fraction which was adjusted empirically from the observed values to make the mean model SST agree with Levitus (1982). K98 examined the effects of holding meridional and zonal winds at their annual mean values, finding that suppressing meridional variability had little effect on annual cycle amplitude in the equatorial region bounded by 120°W and 90°W and within a few degrees of the equator; and that suppressing zonal wind variability resulted in relatively larger differences from the full forcing runs, but that "rms SST differences from the standard

run were not too much larger than the constant meridional wind case." K98 conclude that, to first order, the three-dimensional ocean advective terms in the cold tongue region tend to cancel each other in the annual cycle and "the variations in SST can be described as simply following the variation of net solar radiation at the sea surface (sun minus clouds)."

Borovikov *et al.* (2000) studied the surface heat balance in the equatorial Pacific using a reduced-gravity model (Schopf and Loughe, 1995) consisting of a well-mixed upper layer and nearly-isopycnal lower layers. Surface heat flux was specified using the atmospheric mixed-layer model of Seager *et al.* (1995b) forced with observed, seasonally varying winds (from two sources), air temperature, specific humidity, solar forcing and cloud cover. The character of the surface heat budget was found to depend substantially on longitude. Borovikov *et al.* (2000) summarize that "In the western Pacific the annual cycle of SST is primarily in response to net surface heat flux. In the central basin [165°W–110°W] the magnitude of the zonal advection term is comparable to that of the net surface heat flux. In the eastern basin the role of zonal advection is reduced and the vertical mixing and advection are more important."

Fu and Wang (2001) used a coupled ocean-atmosphere model of intermediate complexity to study the seasonal cycle of SST in the equatorial Pacific. They found that, in the absence of an annual variation in the zonal wind, the annual range of SST averaged over much of the eastern equatorial Pacific (4°N–4°S, 120°–90°W) was only reduced by about 20%. Whereas, when the annual variation of the meridional winds was removed, the amplitude of the annual cycle was reduced by a factor of about 50%. They find that, in this region, meridional wind affects SST mainly by changing evaporation, entrainment, meridional advection, and the mixed layer depth. They also conclude that the "seasonal cycle of the zonal wind component plays a major role in reproducing the westward progression of annual warming."

Table 1 summarizes the numerical model studies of the seasonal cycle of the eastern tropical Pacific ocean described above. The type of model used, the forcing imposed at the surface, and the conclusion about what primarily drives the seasonal cycle of SST are listed for each study. While the seasonal cycle of SST is reproduced quite credibly in every case, the forcings used and the conclusions reached vary widely.

b. Observational studies

The annual cycle of SST and winds in the equatorial Pacific was documented by Horel (1982) who described a longitudinal change in the phase of the annual cycle of SST such that the warmest waters near the Peru coast appear in March, while farther west, the warmest temperatures occur progressively later and with diminished amplitude. Horel found that the annual cycle in surface wind is dominated by meridional migrations of the trade wind belts, with seasonal flow directed into the summer hemisphere (relative to the annual mean) and found than the annual cycle in meridional wind is larger than that of the zonal wind. Mitchell and Wallace (1992), after scrutiny of oceanic and atmospheric data and motivated by the Philander and Pacanowski (1981) results, raised the question of the importance of the meridional stress in tropical Pacific SST evolution. In particular, they speculated

that the increase in the northward surface winds in response to the onset of the northern summer monsoon may be instrumental in re-establishing equatorial cold tongues. Tozuka and Yamagata (2003) have also suggested that the meridional wind mechanism described by Mitchell and Wallace (1992) is a key pacemaker of the annual cycle in the tropical Pacific, though based on analysis of several observed surface marine variables, Wang (1994) has argued against the hypothesis that monsoonal winds, driven by land heating, cause the near-coastal seasonal evolution of eastern equatorial SST. Based on their analysis, Nigam and Chao (1996) argued that, while the equatorial annual cycle in SST is largely generated by meridional wind-induced coastal upwelling east of 110°W, west of this longitude the "SST annual cycle is driven largely by the coupling of zonal winds and SSTs through equatorial upwelling and zonal SST gradient."[5]

Wang and McPhaden's (1999) analysis of Tropical Atmosphere Ocean Array (TAO) buoy array data shows that the heating of the mixed layer by surface heat fluxes at 0°,110°W is mainly balanced by cooling due to the effects of cooler water being entrained into the mixed layer. They found that zonal and meridional advection, surface heating and vertical heat advection each significantly contributed to the seasonal cycle of SST in this region, with the largest terms being the vertical advection and surface heating.[6] Swenson and Hanson (1999) similarly reported that heat storage, heat export by entrainment of upwelled water and heat export by meridional advection mainly determined the annual heat budget in the eastern equatorial Pacific, although they also reported that zonal heat transport is important to the annual cycle. Whereas Wang and McPhaden (1999) found a warming due to meridional advection, Swenson and Hanson (1999) found that meridional currents tend to cool the equatorial eastern Pacific. This discrepancy appears to be a result of the fact that the TAO buoy data examined by Wang and McPhaden resolves the effect of eddy heat transport associated with tropical instability waves (Wang and McPhaden, 1999). Bonjean (2001) used currents from buoy drift and current meter records to estimate that meridional and zonal advection by surface currents are important to the mean heat balance of the central and eastern equatorial Pacific. Bonjean also concludes that the vertical transport of heat must be included to balance net surface heating in the eastern tropical Pacific. Invoking the effects of vertical turbulent mixing, upwelling and TIWs, as inferred from residuals in their mixed layer temperature balance along 95°W, McPhaden *et al.* (2008) found their results to be consistent with a scenario in which "turbulent processes are responsible for mixing cold upwelled water in the surface layer" in late boreal spring (May-June) and that "as meridional winds intensify in June and July, the region of maximum entrainment and minimum SST both shift upwind…", consistent with the effects of meridional winds along the equator discussed by Philander and Pacanowski (1981). This led them to conclude that

5. This led Nigam and Chao (1996) to propose a "westward expansion hypothesis" for the seasonal cycle, with similar dynamics to the "slow SST mode" proposed by Neelin (1991) to explain interannual SST variability [see also Chang and Philander (1994) and Xie (1994) for alternative "westward expansion" hypotheses].

6. See also Hayes *et al.* (1991) for a description of mixed layer heating at 0°,110°W and Enfield (1986) for heat budget estimates over the entire equatorial Pacific.

their "results support the Mitchell and Wallace (1992) hypothesis about the importance of the increase in the northward surface winds…in re-establishing the Pacific equatorial cold tongue during boreal summer."

Estimates of upwelling velocity and mean source temperature of upwelled water are given by Wyrtki (1981) and, more recently, by Johnson *et al.* (2001) who found that, averaged over 3.6°S–5.2°N, 170°E–95°W the upwelling velocity peaked at 1.9 (±0.9) 10^{-5} m/s at 50 m depth, and that, on average, the difference between surface water and source water was 4°C.

Cronin *et al.* (2006) examined the role of clouds in various locations in the far eastern equatorial Pacific. Their analysis of meteorological buoy-based downward longwave and shortwave surface fluxes indicates that, over the cold tongue, cloud forcing is stronger when SST is cool. Clouds reduce incoming shortwave radiation as well as increase downward longwave radiation. Cronin *et al.* found that, over all eastern Pacific regions considered, the shortwave radiation effect is larger than the longwave cloud effect and thus, the net effect of clouds is to increase net downward (into ocean) radiation when SST is warm and cloud cover relatively low in Boreal spring.

3. The model

The model used here is basically the Philander and Seigel (1985) version of the Bryan-Semtner-Cox (Bryan, 1969; Semtner, 1974; Cox, 1984) primitive equation model that Philander and Pacanowski have developed over the past decades (Pacanowski, 1996). It is used here with 27 levels in the vertical. The upper grid point is at 5 m, with a uniform 10 m grid in the upper 100 m, and increasingly nonuniform deeper; there are 17 levels above 250 m. The horizontal grid is uniform between 10°N and 10°S, with 0.33 degree resolution in latitude and 1.0 degree resolution in longitude. Poleward of 10 degrees the meridional resolution increases non-uniformly, to 50°N and to 25°S. Constant horizontal eddy viscosity (A_m) and heat diffusion (A_h) coefficients are used, with $A_m = 10^3\ m^2/s$ and $A_h = 2 \times 10^3\ m^2/s$. Note that our A_m is a factor of two smaller than that used by Philander and Seigel (1985). Subgrid scale mixing in the vertical is done with the Richardson number-dependent mixing formulation described by Pacanowski and Philander (1981). Convective adjustment by the original Bryan formulation will also contribute to vertical mixing if there is sufficient surface cooling. The model was initialized with no motion and with temperature-salinity specified by climatological fields in January (Levitus, 1982). The baseline model $\mathbf{T}^X\mathbf{T}^Y$ (described below) was forced for 15 years by climatological monthly mean surface wind stresses, developed from the COADS[7] marine data set and the Large and Pond (1981) stability-dependent drag coefficient (Harrison, 1989)[8] and by the Philander and Seigel (1985) surface heat flux parameterization as modified by Harrison (1991) and used more recently by Harrison *et al.* (2001a,b) and Harrison and Chiodi (2009). The reference atmospheric temperature field

7. Comprehensive Ocean-Atmosphere Data Set, compiled from ship records (Woodruff *et al.*, 1987).

8. The bulk formula $\tau = \rho_a C_D |u| u$ was used to estimate the surface wind stress vector $\boldsymbol{\tau}$ (τ^x, τ^y) in terms of the wind speed **u** (u,v) at a height of 10 m above the sea surface, the air density ρ_a and drag coefficient C_D. C_D depends on u, so that an iterative process is required to obtain τ.

for use in the surface heat flux calculation is the climatological seasonally varying COADS marine data set used in Philander *et al.* (1987).

a. The surface heat flux boundary condition

In the absence of a coupled model, in which the surface heat flux emerges naturally, the best we can hope for is a form of 'self-consistency,' or compatibility between observations and model predictions. Since we lack direct observational knowledge of vertical velocity (w) and vertical mixing very near the surface, however, we cannot say that any model is right; we can only reconcile it with the observations at hand.

The boundary condition that restores SST to climatology is typically something like:

$$Q = \kappa(SST - T_o) \tag{1}$$

where Q is the heat flux (cal $\mathrm{cm}^{-2}\,\mathrm{s}^{-1}$, defined such that positive Q implies heating of the ocean), T_o is the imposed climatological restoring temperature, and κ is a coupling coefficient. This is the surface heat flux condition that has been criticized by Seager *et al.* (1995a). The basic criticisms are (a) if SST is restored strongly to the seasonal cycle in T_o, SST is fixed by the boundary condition, independent of the model dynamics. In addition, as SST approaches T_o the heat flux goes to zero, which is unphysical, since then the ocean cannot act to transport heat - which we know it does, (b) values for κ required to match data (e.g., Berry and Kent, 2009) are too large, and (c) condition (1) assumes that the atmosphere has an infinite heat capacity,

The response to (a) and (b) above may be formulated by examining the actual surface heat flux boundary condition used in our model, i.e.,

$$Q(x, y, z, t) = SW(x, y, z, t) - LW - QS(x, y, t) - QE(x, y, t) \tag{2}$$

where SW is solar shortwave heating (a function of latitude y, longitude x, and depth z), LW is the longwave back radiation (set to a constant value of $55\,\mathrm{W/m^2}$), QS is the sensible heat flux and QE is the latent heat flux. The only part of (2) that resembles (1) is the sensible heat flux:

$$QS = \rho_a C_e c_{pa} |v| (SST - T_a) \tag{3}$$

where ρ_a is the surface air density, C_e is an exchange coefficient (set to a constant value of 1.4×10^{-3}), c_{pa} is the heat capacity of air (set to a constant value of $1.0 \times 10^3\,\mathrm{J/kg/K}$), and $|v|$ is the wind speed. QS, v, and SST are functions of latitude and longitude, and are computed for each time step. The externally imposed air temperature (T_a) is also a function of latitude and longitude, and is updated for each time step. But QS is relatively small compared to the short wave solar radiation and latent heat components:

$$SW = q_s(r \cdot e^{(-z/\alpha_1)} + (1 - r) \cdot e^{(-z/\alpha_2)}) \tag{4}$$

$$QE = \rho_a C_e L |v| \frac{0.662}{P_{atm}} (e_s(SST) - H_r e_s(T_a)) \tag{5}$$

where q_s is the shortwave incident on ocean surface (which varies in space and time), r is the shortwave partition for near infrared-radiation (0.58 penetrates below 1 m), p_{atm} is atmospheric pressure, and $\alpha_{1,2}$ are e-folding scales for the vertical absorption of the short wave radiation with depth z. The shortwave incident on the ocean surface is parameterized with latitude and cloud cover (which is in turn parameterized with SST according to the methods of Harrison (1991)). In addition, r and $\alpha_{1,2}$ vary with geographic region (warm pool, central-eastern Pacific, far-eastern Pacific), in general agreement with observations. In (5) L is the latent heat of vaporization per unit mass (2.5×10^6 J/kg), H_r is the relative humidity (taken to be 0.8), and $e_s(SST)$ is the saturation vapor temperature.

The boundary condition (2) contains considerably more physics than implied by (1), and is not subject to the constraints about which Seager expresses concern; in this case accurately predicted SST results in accurately predicted turbulent surface fluxes rather than the zero flux condition implied by (1). In this context, κ as defined by (1) is irrelevant. The statement that the SST is fixed by a restoring surface heat flux boundary condition presupposes that near-surface vertical and horizontal advection and diffusion of heat is unimportant. Contrary to this, preliminary examination of this term balance has shown that oceanic advection is of fundamental importance to the annual mean upper ocean heat budget.[9] Thus, the use of bulk formula to couple an ocean model to a climatological atmosphere has assuaged these concerns raised by Seager.

The point (c) above is resolved by comparing the model heat fluxes with observed climatological values (e.g., Berry and Kent, 2009; Zhang *et al.*, 2004; Yu *et al.*, 2004). These observed values presumably do not require an infinite atmospheric heat capacity. For surface heat flux, values derived from observations typically have $\pm 30\,\mathrm{W/m^2}$ errors in Q; we have that level of freedom to work with. As we will show below, the model heat fluxes in the base case agree with observations to zeroth order.

Consideration of model heat fluxes also allows for a more complete evaluation of the experimental results. The specification of air temperature in the QE and QS components of boundary condition (2) does provide some (unrealistic) tendency for SST to track air temperature. Thus, conclusions reached by considering the SSTs produced in the experiments alone can be contaminated by this hidden relaxation effect; however, considering heat fluxes allows experiment configurations that produce reasonable seasonal variations of SST at the cost of imposing unrealistic surface heat fluxes (by imposing air temperature), to be deemed inconsistent with our current understanding of the coupled system. On the other hand, forcings that can be removed, while leaving SST and heat flux behavior largely unchanged, can be said to be of, at best, secondary importance.

9. Support for this is also provided by considering results of Killworth *et al.* (2000) who examined errors in surface tracers and fluxes that occur from the application of (1) to a model similar to that used here and found that a tell-tale phase shift in the seasonal cycle of about a month occurs as a result of these errors. We refer readers to our results section where it is clear that no such phase shift is apparent in the model results discussed here.

Table 1. Summary of the wind stress forcing for the numerical experiments. τ^x and τ^y are zonal and meridional wind stress, respectively. The brackets $\langle\rangle$ denote an annual mean quantity. T_{air}, and I denote that seasonal air temperature and net solar radiation are specified in the surface heat flux boundary condition, respectively; $\langle Q\rangle$ denotes that annual mean surface heat flux (computed in experiment $\mathbf{T^X T^Y}$) is imposed as a constant surface heat flux boundary condition.

Experiment	Wind Stress Components				Heat Flux	
	τ^x	$\langle\tau^x\rangle$	τ^y	$\langle\tau^y\rangle$	T_{air},I Specified	$\langle Q\rangle$ Specified
$\mathbf{T^X T^Y}$	x		x		x	
$\mathbf{T^X}$	x				x	
$\langle\mathbf{T^X}\rangle\mathbf{T^Y}$		x	x		x	
$\langle\mathbf{T^X}\rangle\langle\mathbf{T^Y}\rangle$		x		x	x	
$\mathbf{T^X T^Y}\langle\mathbf{Q}\rangle$	x		x			x

4. The experiments

a. Description of the experiments

The results from five numerical experiments are reported here (the wind stress field characteristics of each experiment are summarized in Table 2). The first experiment (denoted $\mathbf{T^X T^Y}$ for τ^x, τ^y) is the baseline experiment. Both components of the seasonally averaged surface wind stress are imposed, and seasonally averaged air temperature and net solar radiation are specified in the surface heat flux boundary condition. Figure 1 shows the zonal (τ^x) and meridional (τ^y) components of the wind stress fields used to force the model. Figures 1a, 1b show the seasonal cycle of the forcing on the equator; the forcing fields between 10°N and 10°S for March (Figs. 1c,1d) and for September (Figs. 1e,1f) are also shown. The summer intensification of the northward meridional stress, particularly eastward of 170°W, is evident in Figures 1b and 1f.

The results of this baseline experiment have been compared with climatological surface data (SST and surface ship drift) and with equatorial zonal currents at 140°W and 110°W (Harrison *et al.*, 2000); some discrepancies with observations remain, but substantial agreement exists in the annual mean and the seasonal cycle of SST and zonal flow and in the amplitude of the equatorial instability waves. Also, averaged over the equatorial region considered by Johnson *et al.* (2001), the model upwelling velocity at 50 m (1.0×10^{-5} m/s) is in rough agreement (within quoted uncertainty) with their observational estimate.

The remaining experiments indicated in Table 2 begin from the end of the $\mathbf{T^X T^Y}$ experiment, so that at their initiation the model climatological seasonal cycle is fully developed. The second experiment is identical to $\mathbf{T^X T^Y}$ except the meridional wind stress component τ^y is set equal to zero; τ^x is left unchanged and wind speed (needed for latent and sensible heat fluxes) is determined from applied τ and bulk formula (described in Model section above). This experiment will be called $\mathbf{T^X}$.

The third experiment is identical to $\mathbf{T^X T^Y}$ except that the zonal wind stress field τ^x is set equal to its annual mean value ($\langle\tau^x\rangle$, where the brackets denote an annual mean quantity); this experiment will be called $\langle\mathbf{T^X}\rangle\mathbf{T^Y}$. The intent of experiment $\langle\mathbf{T^X}\rangle\mathbf{T^Y}$ is to explore how

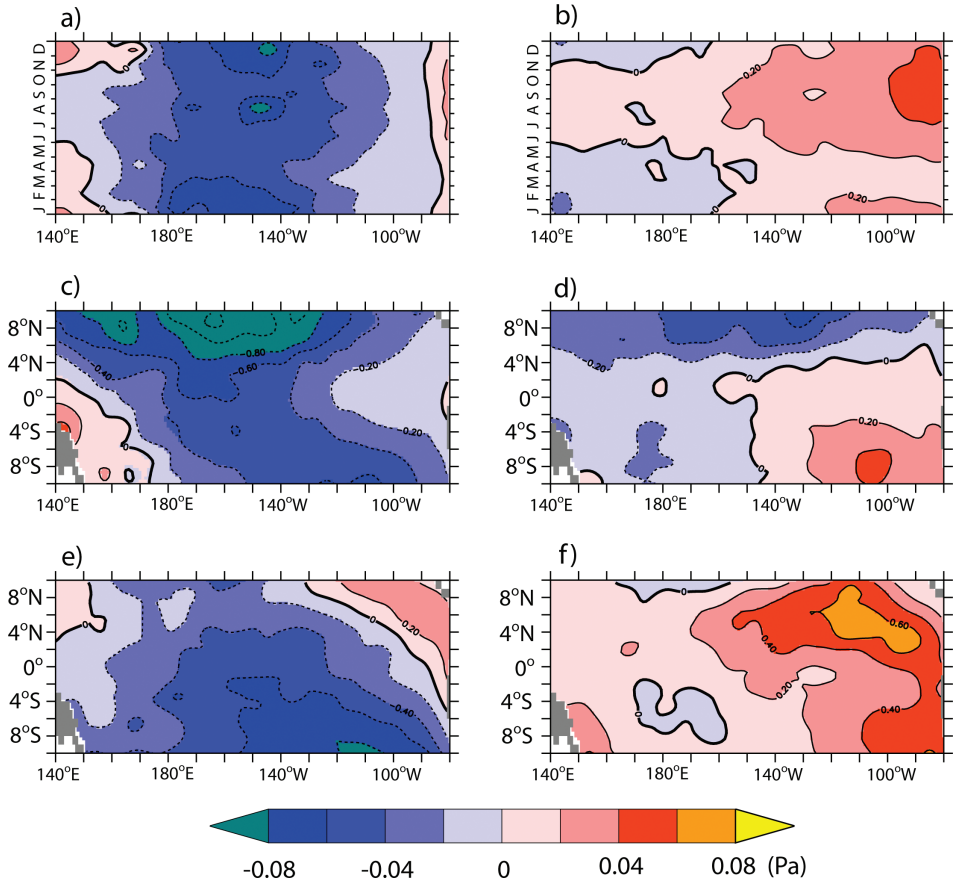

Figure 1. (a) Seasonal cycle of τ^x applied to the model along the equator. (b) Same as (a), for τ^y. (c) March monthly mean τ_x. (d) March monthly mean τ^y. (e) September monthly mean τ_x. (f) September monthly mean τ^y.

much of the seasonal cycle can be reproduced by the meridional wind stress when the large scale zonal structure of the circulation is maintained by the annual mean zonal wind stress field. If τ^x is set equal to zero instead of its annual average, the adjustment involves a large scale collapse of the Pacific zonal temperature gradient (a 'super' el Niño), which masks the seasonal cycle; this experiment is not shown here.

The fourth experiment uses the annual mean zonal and meridional wind stress fields ($\langle\tau^x\rangle$, $\langle\tau^y\rangle$), denoted as $\langle\mathbf{T}^{\boldsymbol{X}}\rangle\langle\mathbf{T}^{\boldsymbol{Y}}\rangle$. The intent of $\langle\mathbf{T}^{\boldsymbol{X}}\rangle\langle\mathbf{T}^{\boldsymbol{Y}}\rangle$ is to examine how much of the seasonal cycle can be reproduced by the imposed seasonally varying atmospheric forcing (e.g., air temperature; solar radiation) with annual mean zonal and meridional wind stress.

The final (fifth) experiment, denoted as $\mathbf{T}^{\boldsymbol{X}}\mathbf{T}^{\boldsymbol{Y}}\langle Q\rangle$, uses the full time-varying wind stress field, but instead of computing the surface heat flux at each time step, imposes a constant

surface heat flux. The constant heat flux used in $\mathbf{T}^X\mathbf{T}^Y\langle Q\rangle$ is the annual mean (but spatially varying) heat flux computed in experiment $\mathbf{T}^X\mathbf{T}^Y$. The intent of $\mathbf{T}^X\mathbf{T}^Y\langle Q\rangle$ is to examine how much of the seasonal cycle in the eastern Pacific can be reproduced from the dynamical effects of wind stress alone.

b. Results of the experiments

First consider the seasonal cycle of SST in the various experiments (Fig. 2); instability wave variability has been largely removed by filtering with a 30 day running average. The smoothed COADS SST is also shown (Fig. 2a). Both the COADS data and all the experiments show the Boreal Springtime weakening of the zonal SST gradient, with warmest temperatures occurring in March and coldest temperatures in September/October in the eastern Pacific. The COADS data show a minimum temperature of 21°C, several degrees colder than the experiments. There is much less seasonal variability in the central and western Pacific, and the data and $\mathbf{T}^X\mathbf{T}^Y$ agree. The $\mathbf{T}^X$, $\langle\mathbf{T}^X\rangle\mathbf{T}^Y$ and $\langle\mathbf{T}^X\rangle\langle\mathbf{T}^Y\rangle$ experiments reproduce most of the aspects of SST variability of the $\mathbf{T}^X\mathbf{T}^Y$ experiment, but temperatures in the far-eastern Pacific ($80-100$°W) are typically one degree warmer than in $\mathbf{T}^X\mathbf{T}^Y$. For $\mathbf{T}^X$, except in the far-eastern Pacific, the zonal stress alone is able to reproduce the essential features of the seasonal cycle of SST. Experiments $\langle\mathbf{T}^X\rangle\mathbf{T}^Y$ and $\langle\mathbf{T}^X\rangle\langle\mathbf{T}^Y\rangle$ are unable to sufficiently generate a SST seasonal cycle west of 140°W, where variations in zonal stress presumably drive the system. The $\langle\mathbf{T}^X\rangle\langle\mathbf{T}^Y\rangle$ experiment, forced only through the surface heat-flux boundary condition, shows very little SST variation west of 120°W and only weak seasonal SST variation at 110°W. Wind stress alone, without a time-varying surface heat flux ($\mathbf{T}^X\mathbf{T}^Y\langle Q\rangle$), produces an SST cycle with temperatures in the western Pacific that are several degrees too warm, and unrealistic SST in the far eastern Pacific. These last two cases suggest that both time varying surface heat flux and wind stress are required to reproduce the seasonal cycle of SST. Either one, acting alone, is insufficient.

Figure 3 shows the monthly-averaged fields of SST between 10°S and 10°N, for the COADS seasonal dataset and for each experiment. Monthly averages are shown for March and September. The $\mathbf{T}^X\mathbf{T}^Y$ results show the strengthening and weakening of the cold tongue, the large changes off the south American coast and the shifting of the warmest western Pacific waters from northern to southern hemisphere that are all characteristic of Tropical Pacific SST variation. The model does not warm as much in the eastern Pacific in Boreal Spring as is suggested in climatological SST COADS data, and minimum temperatures in the cold tongue are about a degree off. $\mathbf{T}^X$ again reproduces all of the major equatorial and western Pacific aspects of $\mathbf{T}^X\mathbf{T}^Y$, but not the behavior off the south American coast. $\langle\mathbf{T}^X\rangle\mathbf{T}^Y$ and $\langle\mathbf{T}^X\rangle\langle\mathbf{T}^Y\rangle$ reproduce the seasonal cycle of SST in the eastern Pacific; in particular, they generate the cold tongue and the September upwelling along the South American coast, however the seasonal cycle of SST is not well represented in the western Pacific. For $\langle\mathbf{T}^X\rangle\langle\mathbf{T}^Y\rangle$ the weakening of both the cold tongue and the coastal upwelling in March is underestimated. The $\mathbf{T}^X\mathbf{T}^Y\langle Q\rangle$ experiment captures the amplitude of the cold tongue west of 110°W, but there is anomalously warm water in the northern hemisphere.

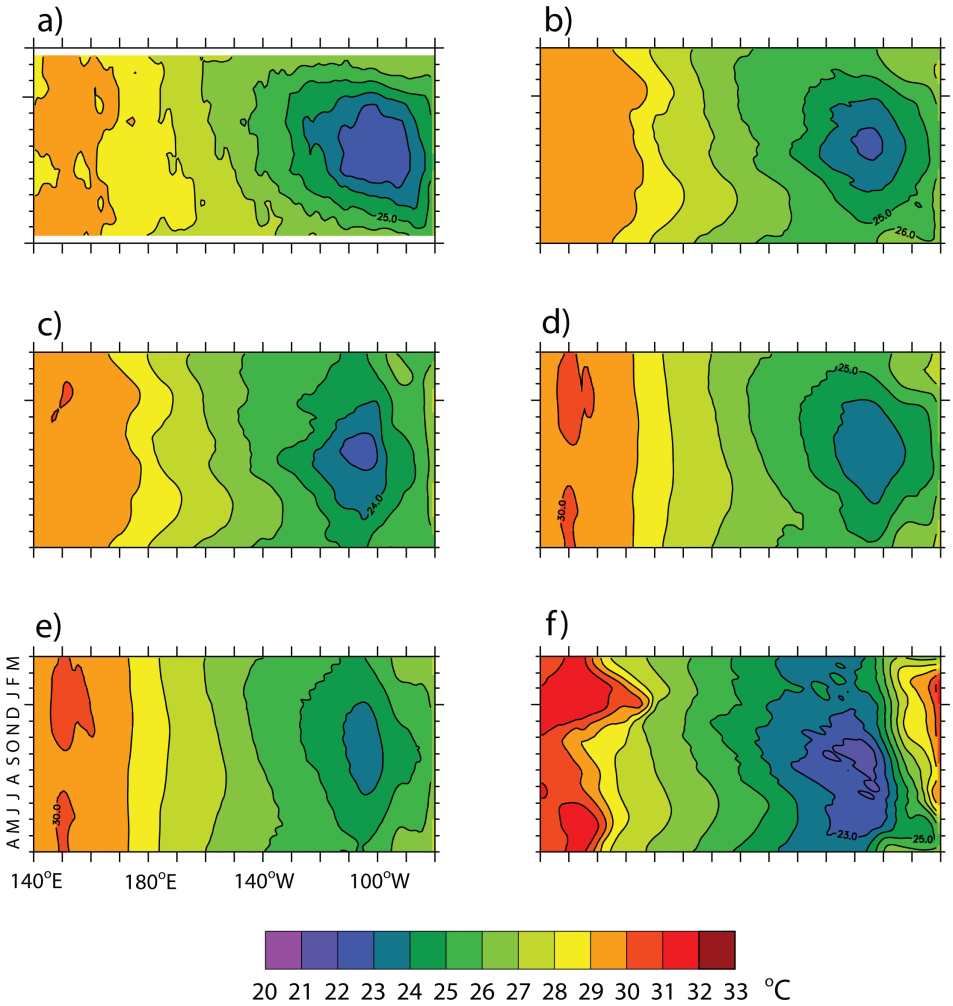

Figure 2. (a) Seasonal cycle of COADS equatorial SST and the seasonal cycle of SST from, (b) the baseline experiment ($\mathbf{T}^X\mathbf{T}^Y$), (c) experiment $\mathbf{T}^X$, (d) experiment $\langle\mathbf{T}^X\rangle\mathbf{T}^Y$, (e) experiment $\langle\mathbf{T}^X\rangle\langle\mathbf{T}^Y\rangle$ and (f) experiment $\mathbf{T}^X\mathbf{T}^Y\langle Q\rangle$.

Now consider the surface heat flux, as computed by the model using (2) and as reported based on COADS data by Berry and Kent (2009) (see also Grist and Josey, 2003), and based on an objectively analyzed-synthesis approach for turbulent fluxes (OAFlux; Yu *et al.*, 2004) and cloud climatology information from the International Satellite Cloud Climatology Project for radiative fluxes (ISCCP; Zhang *et al.*, 2004). Figure 4 shows the seasonal cycle at the equator for the surface heat flux anomaly from the climatological data (Figs. 4a,b) and from the experiments (Figs. 4c–f). To generate the anomaly fields, we have subtracted

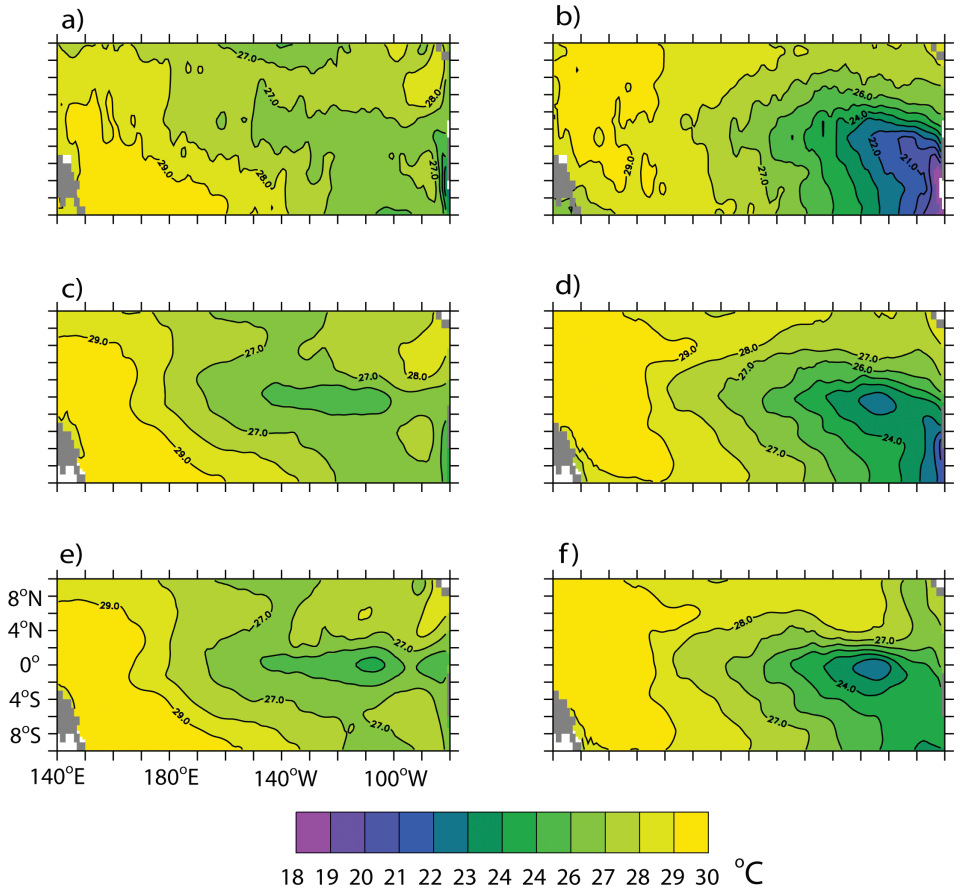

Figure 3. March monthly mean SST from (a) COADS, (c) $\mathbf{T}^X\mathbf{T}^Y$ and (e) $\mathbf{T}^X$. September monthly mean SST from (b) COADS, (d) $\mathbf{T}^X\mathbf{T}^Y$ and (f) $\mathbf{T}^X$.

the annual mean at each grid point. First, note that there is general agreement between the COADS- and OAFlux/ISCCP-based heat fluxes. The $\mathbf{T}^X\mathbf{T}^Y$ and $\mathbf{T}^X$ experiments reproduce the temporal behavior of the seasonal cycle, both in the eastern and western Pacific, in particular the maximum positive departure near the South American coast during Boreal Spring. The remaining experiments ($\langle\mathbf{T}^X\rangle\mathbf{T}^Y$ and $\langle\mathbf{T}^X\rangle\langle\mathbf{T}^Y\rangle$) do not reproduce the seasonal cycle of heat flux in the western Pacific and the location and amplitude of the seasonal cycle in the eastern Pacific. There is considerable reported uncertainty in the COADS data; the $\mathbf{T}^X\mathbf{T}^Y$ heat flux is very close to the COADS data west of 130°W and, while underestimating the heat flux east of 130°W, still falls within one standard deviation of the observations. The $\mathbf{T}^X\mathbf{T}^Y$ model has a net heat flux into the ocean at the equator, verifying that the model can act to transport heat meridionally and vertically as we would expect [criticism (a) above notwithstanding].

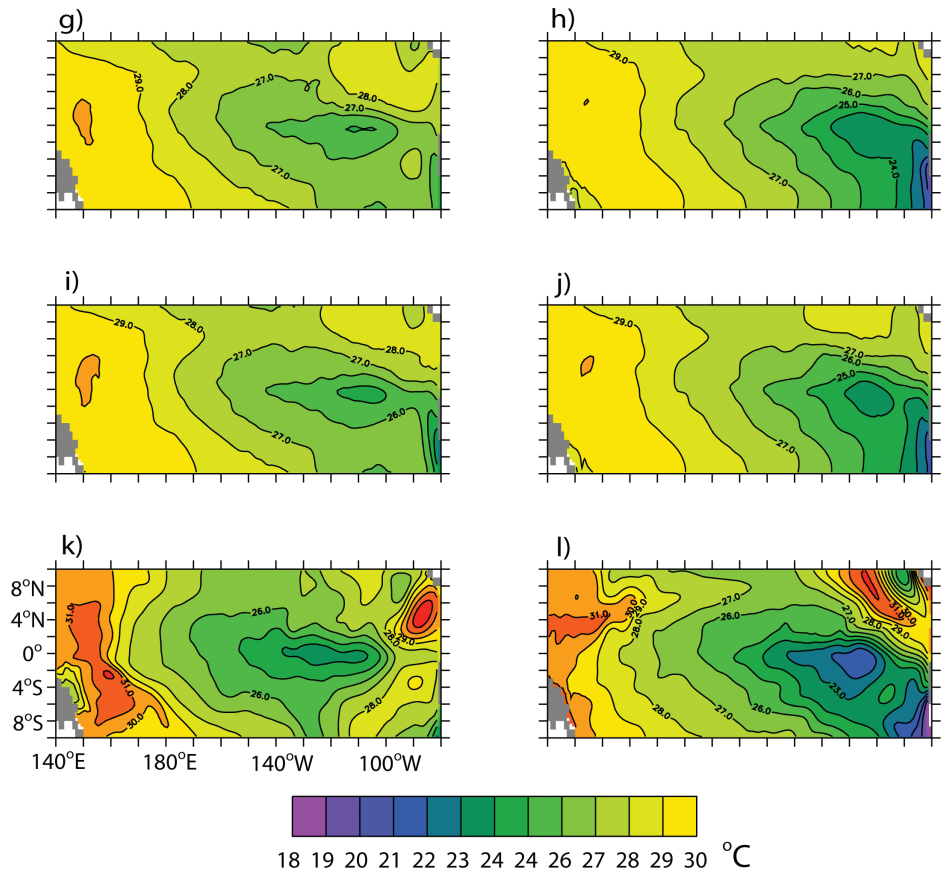

Figure 3. (continued) March monthly mean SST from (g) $\langle \mathbf{T}^X \rangle \mathbf{T}^Y$, (i) $\langle \mathbf{T}^X \rangle \langle \mathbf{T}^Y \rangle$ and (k) $\mathbf{T}^X \mathbf{T}^Y \langle \mathbf{Q} \rangle$. September monthly mean SST from (h) $\langle \mathbf{T}^X \rangle \mathbf{T}^Y$, (j) $\langle \mathbf{T}^X \rangle \langle \mathbf{T}^Y \rangle$ and (l) $\mathbf{T}^X \mathbf{T}^Y \langle \mathbf{Q} \rangle$.

The subsurface zonal currents produced at (140°W, 0°N) by $\mathbf{T}^X \mathbf{T}^Y$ (Fig. 5) agrees well with *in-situ* data from the TAO array. This climatological data, shown in the last panel of Figure 5, was made by monthly-averaging observed zonal velocity from an upward-looking acoustic Doppler profiling current meter (ADCP) mooring at (140°W, 0°N) over the period 1990–1998 (Yu and McPhaden, 1999). This process smooths out the TIWs signature in the TAO data. Note that on these figures, blue colors denote westward flow and red colors denote eastward flow. The seasonal reversal of the normally westward surface flow in late Boreal Spring (March-June), when the TIWs subside and the climatological westward winds are weakest, and when the upper part of the Equatorial Undercurrent (EUC) reaches its maximum speed, is well simulated. The seasonal evolution above the core of the EUC is different from that below the core, also consistent with observations (see Harrison *et al.* (2000), for these comparisons.) Experiments $\mathbf{T}^X$ and $\mathbf{T}^X \mathbf{T}^Y \langle Q \rangle$ reproduce the seasonal cycle

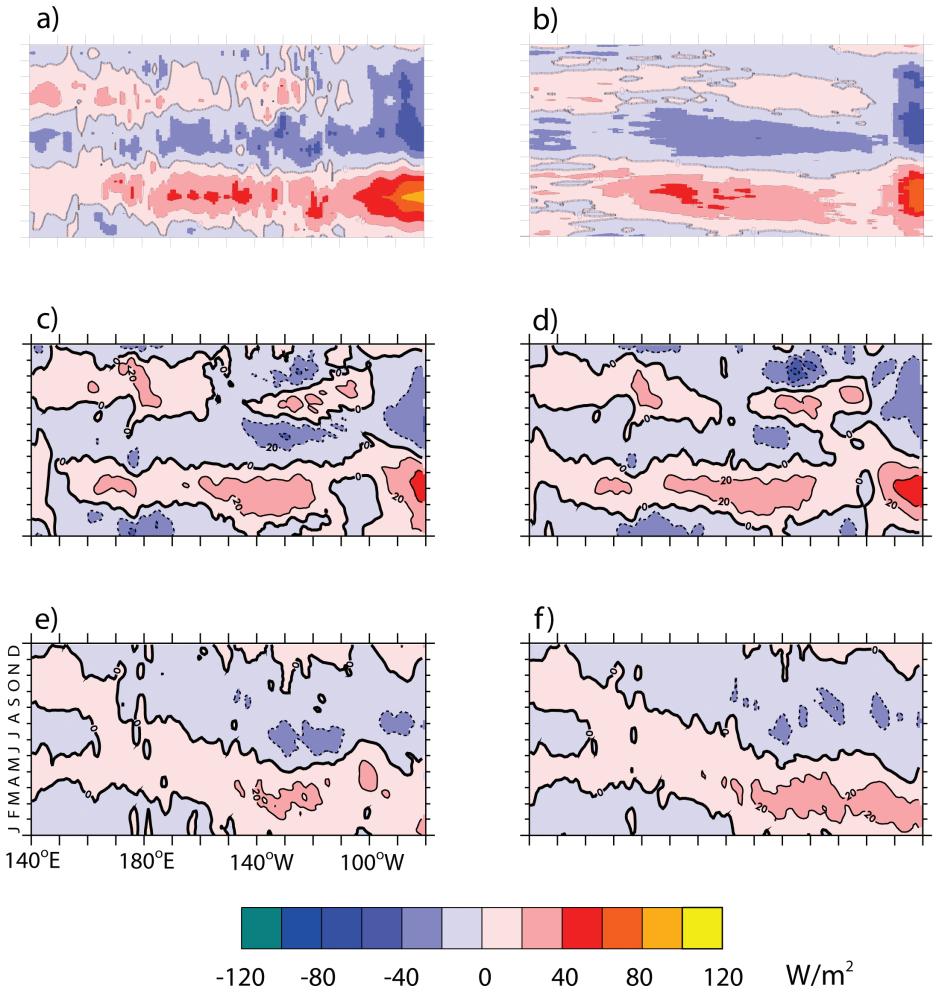

Figure 4. The seasonal cycle of equatorial heat flux from (a) COADS (Berry and Kent, 2009), (b) OAFlux/ISCCP (Zhang *et al.*, 2004; Yu *et al.*, 2004), (c) $\mathbf{T}^X\mathbf{T}^Y$, (d) $\mathbf{T}^X$ and (e) $\langle\mathbf{T}^X\rangle\mathbf{T}^Y$ and (f) $\langle\mathbf{T}^X\rangle\langle\mathbf{T}^Y\rangle$.

of zonal velocity at (140°W, 0°N), consistent with the notion that this process is coupled primarily to the seasonal cycle of zonal wind stress. The apparent lack of impact of τ^y on equatorial zonal flows that can be inferred from these results is perhaps not surprising given known theory for time dependent motion on the equatorial "Beta-plane" (c.f. Sections 4.7 and 4.8 of Philander (1990), and references therein).

Experiments $\langle\mathbf{T}^X\rangle\mathbf{T}^Y$ and $\langle\mathbf{T}^X\rangle\langle\mathbf{T}^Y\rangle$ (forcing by surface heat flux and/or meridional wind stress alone) are unable to reproduce the main features of the seasonal cycle of surface and subsurface currents.

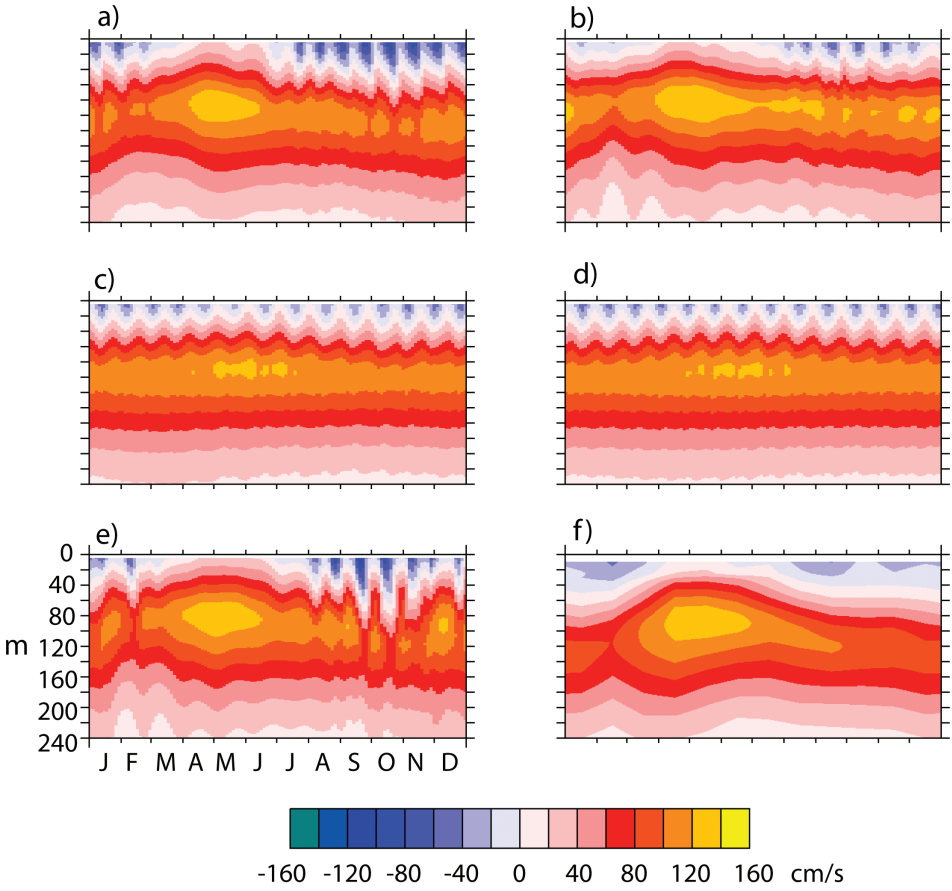

Figure 5. The seasonal cycle of zonal velocity at 140°W, 0°N from (a) $\mathbf{T}^X\mathbf{T}^Y$, (b) $\mathbf{T}^X$ (c) $\langle\mathbf{T}^X\rangle\mathbf{T}^Y$, (d) $\langle\mathbf{T}^X\rangle\langle\mathbf{T}^Y\rangle$, (e) $\mathbf{T}^X\mathbf{T}^Y\langle\mathbf{Q}\rangle$ and (f) TAO data.

This result also extends to the basin-wide seasonal cycle of equatorial surface zonal currents (Fig. 6). $\mathbf{T}^X$ reproduces the basin-wide Boreal Spring and western Pacific Boreal Winter eastward surface current episodes very much as they are seen in $\mathbf{T}^X\mathbf{T}^Y$. As would be expected, $\langle\mathbf{T}^X\rangle\langle\mathbf{T}^Y\rangle$ is unable to reproduce any of the main features of the surface flow in $\mathbf{T}^X\mathbf{T}^Y$; while $\langle\mathbf{T}^X\rangle\mathbf{T}^Y$ approximates the seasonal cycle only in the extreme eastern Pacific; the mechanism for the suppression of the TIWs and the spring current reversal is absent, and TIWs persist all year. $\mathbf{T}^X\mathbf{T}^Y\langle Q\rangle$ generates the seasonal cycle, but the eastward velocity magnitudes are too high in the western part of the basin. Evidently, the lack of a time-varying heat flux requires more transport of heat by near-surface currents.

We may quantify the degree to which the different experiments resemble the 'baseline' experiment ($\mathbf{T}^X\mathbf{T}^Y$) by computing a 'global' or rms error ϵ over a model year in the following way (e.g., for SST):

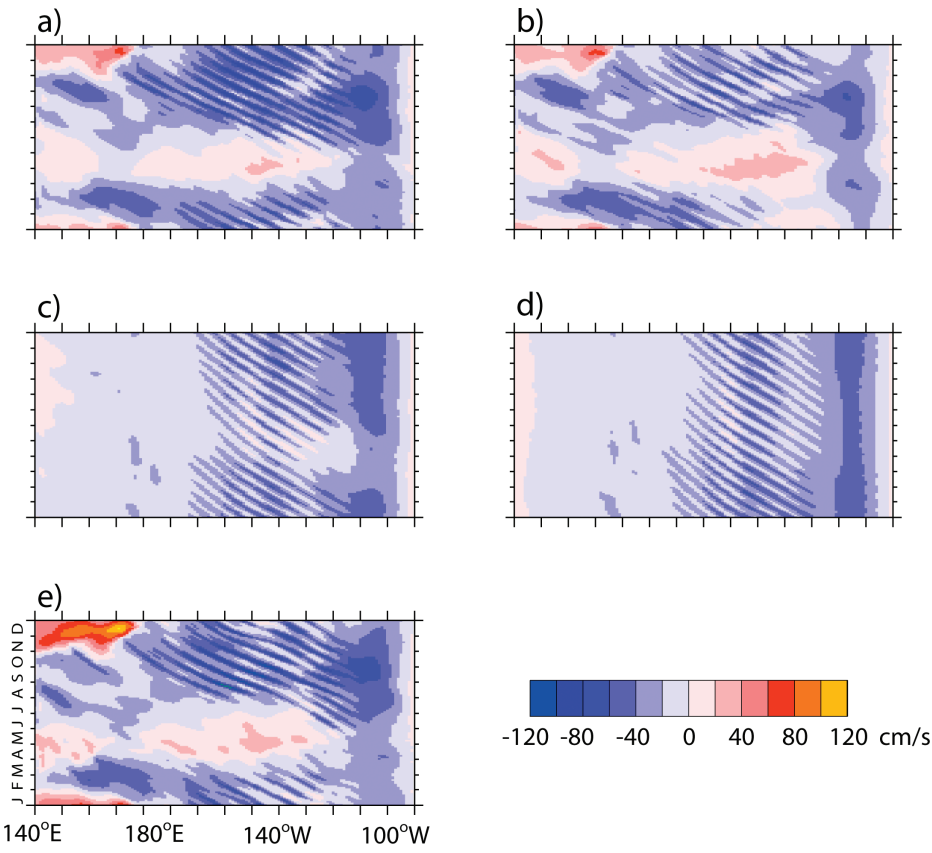

Figure 6. The seasonal cycle of zonal velocity along the equator from (a) $\mathbf{T}^{\boldsymbol{X}}\mathbf{T}^{\boldsymbol{Y}}$, (b) $\mathbf{T}^{\boldsymbol{X}}$ (c) $\langle\mathbf{T}^{\boldsymbol{X}}\rangle\mathbf{T}^{\boldsymbol{Y}}$, (d) $\langle\mathbf{T}^{\boldsymbol{X}}\rangle\langle\mathbf{T}^{\boldsymbol{Y}}\rangle$ and (e) $\mathbf{T}^{\boldsymbol{X}}\mathbf{T}^{\boldsymbol{Y}}\langle\mathbf{Q}\rangle$.

$$\epsilon_{SST} = \frac{1}{N_k}\sum_k \left[\sum_j \sum_i \frac{\left(SST_{ijk} - SST_{ijk}^{T^X T^Y}\right)^2}{N_i N_j}\right]^{1/2} \tag{6}$$

where the i and j sums are taken over the model latitude-longitude grid points, the k sum is taken over time snapshots from a model year, and where N_i, N_j; and N_k represent the number of grid points in latitude, longitude and time, respectively. Table 3 shows the results for SST, zonal velocity and meridional velocity. For each case, grid points at latitudes from 5°S to 5°N were summed, and ϵ was computed for four different longitude regions: the entire equatorial waveguide (131°E-70°W), the western Pacific (west of the dateline: 131°E-180°W), the predominant trade wind region (95°W-180°W), and the extreme eastern Pacific (95°W-70°W). For $\mathbf{T}^{\boldsymbol{X}}$, errors get progressively worse as you go east. For the western Pacific, $\mathbf{T}^{\boldsymbol{X}}$ reproduces $\mathbf{T}^{\boldsymbol{X}}\mathbf{T}^{\boldsymbol{Y}}$ better than the other experiments, but in the extreme eastern Pacific $\mathbf{T}^{\boldsymbol{X}}$ does worse than the experiment with annual mean zonal stress and with either

Table 2. Summary of the average (rms) error ϵ for (a) SST (°C), (b) surface zonal current u (cm/s), and (c) surface meridional currents v (cm/s). The errors were computed with Eq. 6, and represent average deviations from the baseline $\mathbf{T^X T^Y}$ model run for experiments $\mathbf{T^X}$, $\langle \mathbf{T^X} \rangle \mathbf{T^Y}$, $\langle \mathbf{T^X} \rangle \mathbf{T^Y}$ and $\mathbf{T^X T^Y} \langle \mathbf{Q} \rangle$ (A summary of these experiments is listed in Table 2.) For each case, an entire seasonal cycle (model year) was used, grid points at latitudes from 5°S to 5°N were summed, and ϵ was computed for four different longitude regions: (1) the entire equatorial waveguide (131°E-70°W), (2) the western Pacific (west of the dateline: 131°E-180°W), (3) the predominant trade wind region (180°W-95°W), and (4) the extreme eastern Pacific (95°W-70°W).

(a) ϵ_{SST}

	131°E-70°W	131°E-180°W	180°W-95°W	95°W-70°W
$\mathbf{T^X}$	0.45	0.12	0.47	0.78
$\langle \mathbf{T^X} \rangle \mathbf{T^Y}$	0.33	0.23	0.38	0.29
$\langle \mathbf{T^X} \rangle \langle \mathbf{T^Y} \rangle$	0.40	0.27	0.42	0.49
$\mathbf{T^X T^Y} \langle Q \rangle$	1.5	1.2	1.4	2.6

(b) ϵ_u

	131°E-70°W	131°E-180°W	180°W-95°W	95°W-70°W
$\mathbf{T^X}$	15	10	17	10
$\langle \mathbf{T^X} \rangle \mathbf{T^Y}$	18	17	19	7.1
$\langle \mathbf{T^X} \rangle \langle \mathbf{T^Y} \rangle$	19	19	19	3.4
$\mathbf{T^X T^Y} \langle Q \rangle$	15	14	16	7.0

(c) ϵ_v

	131°E-70°W	131°E-180°W	180°W-95°W	95°W-70°W
$\mathbf{T^X}$	15	8.4	18	11
$\langle \mathbf{T^X} \rangle \mathbf{T^Y}$	16	8.8	19	4.8
$\langle \mathbf{T^X} \rangle \langle \mathbf{T^Y} \rangle$	16	10	19	4.9
$\mathbf{T^X T^Y} \langle Q \rangle$	17	10	20	6.8

time-varying ($\langle \mathbf{T^X} \rangle \mathbf{T^Y}$) or annual mean ($\langle \mathbf{T^X} \rangle \langle \mathbf{T^Y} \rangle$) meridional stress included. Experiment $\mathbf{T^X T^Y} \langle Q \rangle$ does considerably worse for SST, but average for reproducing the currents.

5. Conclusions

Although many previous numerical studies of the eastern tropical Pacific (see Table 1) have been able to essentially reproduce the seasonal cycle of SST, there is no consensus for its fundamental cause; different mechanisms have been invoked in each case, and conclusions about the relative importance of different components of the surface forcing are different. Our baseline PE model of the Pacific ($\mathbf{T^X T^Y}$), also reproduces the climatological seasonal cycle of SST well. The $\mathbf{T^X T^Y}$ results show the strengthening and weakening of the cold tongue, the large changes off the south American coast and the shifting of the warmest western Pacific waters from northern to southern hemisphere that are all characteristic of Tropical Pacific SST variation. The subsurface zonal currents produced at (140°W, 0°N) by $\mathbf{T^X T^Y}$ agree well with in-situ data from the TAO array. The seasonal reversal of the normally westward surface flow in late Boreal Spring (March-June), when the TIWs subside and the climatological westward winds are weakest, and when the upper part of the Equatorial

Undercurrent (EUC) reaches its maximum speed, is well simulated. We are not restoring our system any more strongly than others (e.g., Kessler or Seager). Our seasonal cycle experiment ($\mathbf{T}^X\mathbf{T}^Y$) is self-consistent in the sense defined in Section 2 above: forced by the climatological winds, air temperature and solar radiation, the computed surface heat flux, SST, currents and vertical density structure are consistent with climatological observations.

Because the surface heat flux boundary condition is critical in this context, in Section 3 we have discussed the role of our surface heat flux boundary condition in the near-surface heat equation. In particular, we have shown that Seager's criticism of the "Haney-type" boundary condition (Haney, 1971) does not apply. SST emerges as an independent quantity in our model.

In a series of numerical experiments where we have removed elements of the atmospheric forcing, we find that the different cases all produce relatively realistic seasonal cycles of SST. Although the SST signal is quite robust, due partly to the imposition of climatological air temperature in the applied surface boundary condition, only the most complete model is also able to reproduce the seasonal cycle of near surface currents and tropical instability waves (TIWs) with consistent heat fluxes.

The $\langle\mathbf{T}^X\rangle\mathbf{T}^Y$ and $\langle\mathbf{T}^X\rangle\langle\mathbf{T}^Y\rangle$ experiments reproduce most aspects of SST variability seen in the $\mathbf{T}^X\mathbf{T}^Y$ experiment, but they do so only with the imposition of surface heat fluxes that are largely inconsistent with the observation-based estimates of surface heat fluxes considered here (including in the eastern Pacific.) On the other hand, we have found that a model simulation made with the zonal wind stress alone ($\mathbf{T}^X$) reproduces very well the equatorial seasonal behavior (e.g., in SST and surface heat fluxes) of the climatological experiment ($\mathbf{T}^X\mathbf{T}^Y$), except in the far eastern Pacific (east of 100°W). Thus, the effects of meridional stress are not negligible, but neither are they crucial. In this sense, the experiments confirm some results reported by Kessler *et al.* (1998), which demonstrate the importance of other forcings such as zonal wind stress and surface heat flux, but repudiate others that emphasize the role of meridional winds, such as the idea from Takeuchi (1986) that meriodional winds along the coast of S. America provide the main source of cold water to the equatorial cold tongue region, or the arguments of Mitchell and Wallace (1992; discussed more below). Additionally, the simultaneous consideration of SST and surface heat flux has shown zonal stress variations to be the more fundamental forcing function in the context of the experiments described here. For $\mathbf{T}^X$, errors get progressively worse as you go east. For the western Pacific, $\mathbf{T}^X$ reproduces $\mathbf{T}^X\mathbf{T}^Y$ better than the other experiments, but in the extreme eastern Pacific $\mathbf{T}^X$ does worse than the experiment with annual mean zonal stress and with either time-varying ($\langle\mathbf{T}^X\rangle\mathbf{T}^Y$) or annual mean ($\langle\mathbf{T}^X\rangle\langle\mathbf{T}^Y\rangle$) meridional stress included.

Wind stress alone, without a time-varying surface heat flux ($\mathbf{T}^X\mathbf{T}^Y\langle Q\rangle$) produces an SST cycle with temperatures in the western Pacific that are several degrees too warm, and unrealistic SST in the far eastern Pacific. In this case, however, currents are still reproduced reasonably. Thus, currents are forced mainly by wind stress, while the seasonal cycle of SST depends strongly on seasonal variations in surface heat flux.

A model simulation made with the annual mean winds, forced only through the surface heat-flux boundary condition ($\langle \mathbf{T}^X \rangle \langle \mathbf{T}^Y \rangle$) generates a seasonal cycle of SST that is superficially in agreement with data; in particular, it generates the cold tongue and the September upwelling along the South American coast. However, the seasonal cycle of SST is not well represented west of 120°W, and this case does not yield consistent heat fluxes or currents. In the absence of seasonally varying currents, this system is forced relatively strongly by the seasonal cycle of air temperature, and tropical instability waves are present all year long and presumably are largely responsible for the required heat transfer. These last two cases ($\mathbf{T}^X \mathbf{T}^Y \langle Q \rangle$ and $\langle \mathbf{T}^X \rangle \langle \mathbf{T}^Y \rangle$) suggest that both time varying surface heat flux and wind stress are required to reproduce the seasonal cycle of SST. Either one, acting alone, is insufficient.

Including the annual mean zonal wind stress and the seasonally varying meridional wind stress ($\langle \mathbf{T}^X \rangle \mathbf{T}^Y$) appears to reproduce the September $\mathbf{T}^X \mathbf{T}^Y$ cold tongue. In particular this is the only case (other than the baseline $\mathbf{T}^X \mathbf{T}^Y$) that generates cold upwelled water off the South American coast. The cold tongue, however, does not get advected westward as much as required. $\langle \mathbf{T}^X \rangle \mathbf{T}^Y$ does not adequately simulate either the surface heat flux or the surface equatorial zonal flow. While the mean large scale structure of the subsurface zonal flow field is maintained by the mean zonal stress, the varying meridional stress does not drive much seasonal variation in these fields.

In a seminal study, Philander and Pacanowski (1981) showed that switching on a uniform northward wind stress (0.05 Pa) over a resting ocean produced a pool of cool water in the southeastern part of the rectangular domain, and an equatorial cold tongue with a significant meridional temperature gradient just north of the equator. They further showed that forcing with meridionally uniform but time-varying (zero to 0.1 Pa over a period of 200 days) northward winds, in the eastern part of the basin, can also maintain a somewhat weaker cold tongue. From these results, which did not consider effects of other surface forcing components, they suggested that the meridional winds alone may be responsible for much of the observed seasonal SST variability in the eastern equatorial Atlantic and Pacific ocean. Since this study, a number of authors have made similar claims for the Pacific (e.g., Mitchell and Wallace, 1992; McPhaden *et al.*, 2008) and much effort has been directed toward understanding the influence of meridional winds. In contrast to this perspective, we find that the zonal stress alone drives much of the observed SST variability in the eastern Pacific. In our model, the cold tongue is reestablished without τ^y (i.e., experiment $\mathbf{T}^X$.) These results provide guidance for current efforts to evaluate and develop realistic coupled air-sea models. Recently, de Szoeke and Xie (2008) have drawn attention to the effects that errors in τ^y have on the seasonal cycle of equatorial Pacific SST in coupled air-sea models. Results of our study suggest that, while consideration of τ^y is warranted and perhaps pertinent to the models considered by de Szoeke and Xie (2008), realistic coupled model behavior should be at least as sensitive to variability (errors or otherwise) in τ^x as τ^y, and thus, in order to be realistic, it will be fundamentally important for such models to predict accurate zonal winds.

While the discussion about the relative importance of the surface heat flux and meridional wind stress field in the seasonal cycle of SST will undoubtedly continue, and perhaps be

assisted by future coupled ocean-atmosphere experiments, the experiments reported here indicate that the upper ocean equatorial fields in this ocean circulation model are largely zonal wind stress driven. Meridional stress has little effect except in the easternmost Pacific. More importantly, we have shown that merely reproducing the seasonal cycle of SST does not allow conclusions about dynamics and forcing mechanisms to be made. This leads to the disconcerting notion that using a standard approach, i.e., using a hierarchy of models, starting with the simplest and moving toward more realism as understanding is gained, may be inappropriate.

Acknowledgments. The Ferret analysis program was used in the analysis of the model outputs (http://ferret.pmel.noaa.gov/Ferret/home). This manuscript has benefited from the constructive comments of two anonymous reviewers. This is PMEL contribution #2913 and JISAO publication #1600.

REFERENCES

Arakawa, A. 2004. The cumulus parameterization problem: past, present and future J. Climate, *17*, 2493–2525.

Berry, D. I. and E. C. Kent. 2009. A new air-sea interaction gridded dataset from ICOADS with uncertainty estimates. Bull. Amer. Meteor. Soc., *90*, 645–656.

Bonjean, F. 2001. Influence of surface currents on the sea surface temperature in the tropical Pacific Ocean. J. Phys. Oceanogr., *31*, 943–961.

Borovikov, A., M. M. Rienecker and P. S. Schopf. 2000. Surface heat balance in the equatorial Pacific ocean: climatology and the warming event of 1994–1995. J. Climate, *14*, 2624–2641.

Bryan, K. 1969. A numerical method for the study of the circulation of the World Ocean. J. Comput. Phys., *4*, 347–376.

Cai, M. 2002. Formation of the cold tongue and ENSO in the equatorial Pacific basin. J. Climate, *16*, 144–155.

Cai, W., M. A. Collier and H. B. Gordon. 2003. Strong ENSO variability and a super-ENSO pair in the CSIRO Mark 3 Coupled Climate Model. Mon. Wea. Rev., *131*, 1189–1210.

Cane, M. A. 1979. Response of an equatorial ocean to simple wind stress patterns, 1: Model formulation and analytic results. J. Mar. Res., *37*, 233–252.

Cane, M. A., A. J. Busalacchi and L. M. Rothstein. 1994. The roles of vertical mixing, solar radiation and wind stress in a model simulation of the sea surface temperature seasonal cycle in the tropical Pacific Ocean. J. Geophys. Res., *99*, 20345–20359.

Chang, P. 1994. A study of the seasonal cycle of sea surface temperature in the tropical Pacific Ocean using reduced gravity models. J. Geophys. Res., *99*, 7725–7741.

——— 1996. The role of the dynamic ocean-atmosphere interactions in the tropical seasonal cycle. J. Climate, *9*, 2973–2985.

Chang, P. and S. G. H. Philander. 1994. A coupled ocean-atmosphere instability of relevance to the seasonal cycle. J. Atmos. Sci., *51*, 3627–3648.

Chen, D., L. M. Rothstein and A. J. Busalacchi. 1994a. A hybrid vertical mixing scheme and its application to tropical ocean models. J. Phys. Oceanogr., *24*, 7725–7741.

Chen, D., A. J. Busalacchi and L. M. Rothstein. 1994b. The role of vertical mixing, solar radiation, and wind stress in a model simulation of the sea-surface temperature seasonal cycle in the tropical Pacific Ocean. J. Geophys. Res., *99*, 20345–20359.

Cox, M. D. 1984. A Primitive Equation, 3-Dimensional Model of the Ocean, GFDL Ocean Group Technical Report No. 1. 143 pp.

Cronin, M. F., N. A. Bond, C. W. Fairall and R. A. Weller. 2006. Surface cloud forcing in the east Pacific stratus deck/cold tongue/ITCZ complex. J. Climate, *19*, 392–409.

Davey M. K., M. Huddleston, K. R. Sperber and the Model Data Contributors. 2002. STOIC: A study of coupled model climatology and variability in tropical ocean regions. Climate Dyn., *18*, 403–420.

Delecluse, P., M. K. Davey, Y. Kitamura, S. G. H. Philander, M. Suarez and L. Bengtsson. 1998. Coupled general circulation modeling of the tropical Pacific. J. Geophys. Res., *103*, 14357–14373.

de Szoeke, S. P. and S. -P. Xie. 2008. The tropical eastern Pacific seasonal cycle: assessment of errors and mechanisms in IPCC AR4 coupled ocean-atmosphere general circulation models. J. Climate, *21*, 2573–2590.

DeWitt, D. G. and E. K. Schneider. 1999. The processes determining the annual cycle of equatorial sea surface temperature: A coupled general circulation model perspective. Mon. Wea. Rev., *127*, 381–395.

Enfield, D. B. 1986. Zonal and seasonal variations of the near-surface heat balance of the equatorial Pacific Ocean. J. Phys. Oceanogr., *16*, 1038–1054.

Fu, X. and B. Wang. 2001. A coupled modeling study of the seasonal cycle of the Pacific Cold Tongue, Part I: Simulation and sensitivity experiments. J. Climate, *14*, 765–779.

Gent, P. R. and M. A. Cane. 1989. A reduced gravity, primitive equation model of the upper Equatorial Ocean. J. Comput. Phys., *81*, 444–480.

Giese, B. and J. Carton. 1994. The seasonal cycle in a coupled ocean-atmosphere model. J. Climate, *7*, 1208–1217.

Gordon, C. and R. A. Corry. 1991. A model simulation of the seasonal cycle in the tropical Pacific Ocean. J. Geophys. Res, *96*, 847–864.

Grist, J. P. and S. A. Josey. 2003. Inverse analysis adjustment of the SOC air-sea flux climatology using ocean heat transport constraints. J. Climate, *20*, 3274–3295.

Guilyardi, E. 2006. El Niño-mean state-seasonal cycle interactions in a multi-model ensemble. Climate Dyn., *26*, 329–348.

Haney, R. L. 1971. Surface thermal boundary conditions for ocean circulation models. J. Phys. Oceanogr., *1*, 241–248.

Harrison, D. E. 1989. On climatological monthly mean wind stress and wind stress curl fields over the world ocean. J. Climate, *2*, 57–70.

——— 1991. Equatorial sea surface temperature sensitivity to net surface heat flux: Some ocean circulation model results. J. Climate, *4*, 539–549.

Harrison, D. E. and A. M. Chiodi. 2009. Pre- and post-1997/1998 westerly wind events and equatorial Pacific cold tongue warming. J. Climate, *22*, 568–581.

Harrison, D. E., R. D. Romea and S. H. Hankin. 2001. Central equatorial Pacific zonal currents. I: The Sverdrup balance, nonlinearity and tropical instability waves. Annual mean dynamics. J. Mar. Res., *59*, 895–919.

Harrison, D. E., R. D. Romea and G. A. Vecchi. 2001. Central equatorial Pacific zonal currents. II: The seasonal cycle and the boreal spring surface eastward surge. J. Mar. Res., *59*, 921–948.

Harrison, D. E., G. A. Vecchi and R. H. Weisberg. 2000. Eastward surface jets in the central equatorial Pacific, November 1992–March 1992. J. Mar. Res., *58*, 735–754.

Hayes, S. P., P. Chang and M. J. McPhaden. 1991. Variability of the sea surface temperature in the eastern equatorial Pacific during 1986–1988. J. Geophys. Res., *96*, 10553–10566.

Horel, J. D. 1982. On the annual cycle of the tropical Pacific atmosphere and ocean. Mon. Wea. Rev., *110*, 1863–1878.

Johnson, G. C., M. J. McPhaden and E. Firing. 2001. Equatorial Pacific Ocean horizontal velocity, divergence and upwelling. J. Phys. Oceanogr., *31*, 839–849.

Kessler, W. S., L. M. Rothstein and D. Chen. 1998. The annual cycle of SST in the eastern tropical Pacific, diagnosed in an ocean GCM. J. Climate, *11*, 777–799.

Killworth, P. D., D. A. Smeed and A. J. G. Nurser. 2000. The effects on ocean models of relaxation toward observations at the surface. J. Phys. Oceanogr., *30*, 160–174.

Köberle, C. and S. G. H. Philander. 1994. On the processes that control seasonal variations of sea surface temperatures in the tropical Pacific Ocean. Tellus, *46*A, 481–496.

Kraus, E. B. and J. S. Turner. 1967. A one-dimensional model of the seasonal thermocline. II: The general theory and its consequences. Tellus, *19*, 98–105.

Large, W. and S. Pond. 1981. Open ocean momentum flux measurements in moderate to strong winds. J. Phys. Oceanogr., *11*, 324–336.

Latif, M. 1987. Tropical ocean circulation experiments. J. Phys. Oceanogr., *17*, 246–263.

Latif, M. and co-authors. 2001. ENSIP: The El Niño Simulation Intercomparison Project. Climate Dyn., *18*, 255–276.

Levitus, S. 1982. Climatological Atlas of the World Ocean. NOAA Professional Paper 13, U.S. Government Printing Office, Washington, DC, 173 pp.

——— 1987. A comparison of the annual cycle of two sea surface temperature climatologies of the World Ocean. J. Phys. Oceanogr., *17*, 197–214.

Li, T. and S. G. H. Philander. 1996. On the annual cycle of the eastern equatorial Pacific. J. Climate, *9*, 2986–2998.

Lindzen, R. S. and S. Nigam. 1987. On the role of sea-surface temperature gradients in forcing low-level winds and convergence in the Tropics. J. Atmos. Sci., *44*, 2418–2436.

McPhaden, M. J., M. F. Cronin and D. C. McClurg. 2008. Meridional structure of the seasonally varying mixed layer temperature balance in the eastern tropical Pacific. J. Climate, *21*, 3240–3260.

Mechoso, C. S. and Coauthors. 1995. The seasonal cycle over the tropical Pacific in coupled ocean-atmosphere General Circulation Models. Mon. Wea. Rev., *123*, 2825–2838.

Mitchell, T. P. and J. M. Wallace. 1992. On the annual cycle in equatorial convection and sea surface temperature. J. Climate, *5*, 1140–1156.

Neelin, J. D. 1991. The slow sea surface temperature mode and the fast-wave limit: Analytic theory for tropical interannual oscillations and experiments in a hybrid coupled model. J. Atmos. Sci., *48*, 584–606.

Nigam, S. and Y. Chao. 1996. Evolution dynamics of tropical ocean-atmosphere annual cycle variability. J. Climate, *9*, 3187–3205.

Pacanowski, R. C. 1995. MOM 2 documentation, user's guide and reference manual, Version 1.0, GFDL Ocean Group Tech. Rep. 3, 232 pp.

Pacanowski, R. C. and S. G. H. Philander. 1981. Parameterization of vertical mixing in numerical models of tropical oceans. J. Phys. Oceanogr., *11*, 1443–1451.

Perigaud, C., F. Melin and C. Cassou. 2000. ENSO simulated by intermediate coupled models and evaluated with observations over 1970–98. Part I: Role of the off-equatorial variability. J. Climate, *13*, 1605–1634.

Philander, S. G. H. 1990. El Niño, La Niña, and the Southern Oscillation, Academic Press, 293 pp.

Philander, S. G. H., W. J. Hurlin and A. D. Seigel. 1987. Simulation of the seasonal cycle of the tropical Pacific Ocean. J. Phys. Oceanogr., *17*, 1986–2002.

Philander, S. G. H. and R. C. Pacanowski. 1981. The oceanic response to cross-equatorial winds (with application to coastal upwelling in low latitudes). Tellus, *33*, 201–210.

Philander, S. G. H. and A. D. Seigel. 1985. Simulation of El Niño of 1982–1983. *in* Coupled Ocean-Atmosphere Models, J. Nihoul, ed., Elsevier, 517–541.

Price, J. F., R. A. Weller and R. Pinkel. 1986. Diurnal cycling: Observations and models of the upper ocean response to diurnal heating cooling and wind mixing. J. Geophys. Res., *91*, 8411–8427.

Robertson, A. W., C. -C. Ma, C. R. Mechoso and M. Ghil. 1995. Simulation of the tropical Pacific climate with a coupled ocean atmosphere general circulation model. Part I: The seasonal cycle. J. Climate, *8*, 1178–1198.

Schneider, E. K. 2002. Understanding differences between the equatorial Pacific as simulated by two coupled GCMs. J. Climate, *15*, 449–469.

Schopf, P. S. and A. Loughe. 1995. A reduced-gravity isopycnal ocean model: Hindcasts of El Niño. Mon. Wea. Rev., *3*, 2839–2863.

Seager, R. 1989. Modeling tropical Pacific sea surface temperature: 1970–98. J. Phys. Oceanogr., *19*, 419–434.

Seager, R. and B. Blumenthal. 1994. Modeling tropical Pacific sea surface temperature with satellite-derived solar radiative forcing. J. Climate, *7*, 1943–1957.

Seager, R., M. B. Blumenthal and Y. Kushnir. 1995b. An advective atmospheric mixed layer model for ocean modeling purposes: global simulation of surface heat fluxes. J. Climate, *8*, 1951–1964.

Seager, R., Y. Kushnir, and M. A. Cane. 1995a. On heat flux boundary conditions for ocean models. J. Phys. Oceanogr., *25*, 3219–3230.

Seager, R. S. E. Zebiak and M. A. Cane. 1988. A model of the tropical Pacific sea surface temperature climatology. J. Geophys. Res., *93*, 1265–1280.

Semtner, A. J. 1974. An Oceanic General Circulation Model with Bottom Topography, UCLA Dept. of Meteorology Tech. Rep. No. 9, 99 pp.

Swenson, M. S. and D. V. Hansen. 1999. Tropical Pacific Ocean mixed layer heat budget: The Pacific cold tongue. J. Phys. Oceanogr., *29*, 69–81.

Takeuchi, K. 1986. Numerical study of the seasonal variations of the subtropical front and the subtropical countercurrent. J. Phys. Oceanogr., *16*, 919–926.

Tozuka, T. and T. Yamagata. 2003. Annual ENSO. J. Phys. Oceanogr., *33*, 1564–1578.

Wang, B. 1994. On the annual cycle in the tropical eastern central Pacific. J. Climate, *7*, 1926–1942.

Wang, B. and Fu, X. 2001. Processes determining the rapid reestablishment of the equatorial Pacific cold tongue/ITCZ complex. J. Climate, *14*, 2250–2265.

Wang, W. and M. J. McPhaden. 1999. The surface layer heat balance in the equatorial Pacific Ocean, Part I: Mean seasonal cycle. J. Phys. Oceanogr., *29*, 1812–1831.

Wittenberg, A. T., A. Rosati, N. -C. Lau and J. J. Ploshay. 2006. GFDL's CM2 global coupled climate models. Part III: Tropical Pacific climate and ENSO. J. Climate, *19*, 698–722.

Woodruff, S. D., R. J. Slutz, R. L. Jenne and P. M. Steurer. 1987. A comprehensive ocean-atmosphere data set. Bull. Amer. Meteor. Soc., *68*, 1239–1250.

Wyrtki, K. 1981. An estimate of equatorial upwelling in the Pacific. J. Phys. Oceanogr., *11*, 1205–1214.

Xie, S. -P. 1994. On the genesis of the equatorial annual cycle. J. Climate, *7*, 2008–2013.

Yu. L., R. A. Weller and B. Sun. 2004. Improving latent and sensible heat flux estimates for the Atlantic Ocean (1988–1999) by a synthesis approach. J. Climate, *17*, 373–393.

Yu, X. and M. J. McPhaden. 1999. Seasonal variability in the equatorial Pacific. J. Phys. Oceanogr., *29*, 925–947.

Zebiak, S. E. and M. A. Cane. 1987. A Model El-Niño Southern Oscillation. Mon. Wea. Rev., *115*, 2262–2278.

Zhang, Y.-C., W. B. Rossow, A. A. Lacis, V. Oinas, and M. I. Mishchenko. 2004. Calculation of radiative fluxes from the surface to top of atmosphere based on ISCCP and other global data sets: Refinements of the radiative transfer model and the input data. J. Geophys. Res., *109*, doi:10.1029/2003JD004457.

Received: *30 June, 2009*; revised: *15 January, 2010*.